

# The response of Southern Ocean eddies to increased midlatitude westerlies: A non-eddy resolving model study

M. Hofmann<sup>1</sup> and M. A. Morales Maqueda<sup>2</sup>

Received 26 October 2010; revised 10 December 2010; accepted 28 December 2010; published 3 February 2011.

[1] The midlatitude westerlies of the southern hemisphere have intensified since the 1970s. Non-eddy resolving general circulation models respond to such wind intensification with steeper isopycnals, a faster Antarctic Circumpolar Current (ACC), and a stronger Atlantic Meridional Overturning Circulation (AMOC). However, hydrographic observations show little change in the slope of the Southern Ocean isopycnals over the past 40 years. This insensitivity seems to result from a compensating mechanism whereby an initial increase in the slope of the isopycnals causes eddy activity to intensify and forces the isopycnal slopes down. Climate models do not yet resolve ocean eddies, and the eddy parameterizations included in them do not capture well the compensation mechanism mentioned above. We present simulations with a non-eddy resolving model incorporating an eddy parameterization in which eddy compensation is greatly enhanced by the use of a non-constant, spatially varying thickness diffusivity. The sensitivity of the simulated ACC and AMOC to increased southern hemisphere westerlies is greatly reduced compared to simulations using constant and uniform diffusivities. **Citation:** Hofmann, M., and M. A. Morales Maqueda (2011), The response of Southern Ocean eddies to increased midlatitude westerlies: A non-eddy resolving model study, *Geophys. Res. Lett.*, 38, L03605, doi:10.1029/2010GL045972.

## 1. Introduction

[2] Strong westerly winds cause equatorward Ekman transport and deep water upwelling in the area of the ACC [Toggweiler and Samuels, 1998; Wunsch and Ferrari, 2004]. This upwelling is responsible for the density structure of the ACC, with steep isopycnals that connect the deep ocean with the surface mixed layer. This is one of the few regions of the ocean where such direct communication between upper and deep ocean occurs. For this reason, the ACC region is very important for global atmosphere-ocean heat and CO<sub>2</sub> exchanges [Rintoul et al., 2001; Thompson, 2008].

[3] The Southern Annular Mode has evolved during the past four decades towards a state with intensified westerlies [Thompson and Solomon, 2002; Marshall, 2003; Jacobs, 1997]. In non-eddy resolving Ocean General Circulation Models (OGCMs), a strengthening of the Southern Ocean westerlies leads to enhanced northward Ekman transport,

steeper isopycnals, and a stronger ACC [Fyfe and Saenko, 2006; Bi et al., 2002; Saenko et al., 2005]. It has been argued that the increase in poleward deep flow needed to compensate for a larger equatorward Ekman transport at the surface must be accompanied by a strengthening of the AMOC [Toggweiler et al., 1989a, 1989b]. This link between southern hemisphere westerlies and AMOC has so far been found only in OGCMs with low diapycnal diffusivities [Toggweiler and Samuels, 1998]. Gnanadesikan [1999] developed an insightful theory linking the AMOC with the two competing contributions of Ekman transport and eddy effects in the Southern Ocean. This theory was further explored by Hallberg and Gnanadesikan [2001] with an idealized channel model.

[4] Böning et al. [2008] have recently investigated the impact of the changes in surface fluxes observed during the past 50 years on the density structure of the ACC. A surprising result of their study is the absence of noticeable changes in the slope of the isopycnals in response to the strengthening of the westerlies. They attribute this insensitivity to the enhanced poleward eddy transport, that counterbalances the also larger northward Ekman flow. This mechanism of eddy compensation, or saturation, was first advanced by Straub [1993], and is confirmed by several eddy resolving and eddy permitting simulations [e.g., Farneti et al., 2010; Hogg et al., 2008; Hallberg and Gnanadesikan, 2006].

[5] We investigate eddy compensation in a non-eddy resolving OGCM with a time-dependent, three-dimensional eddy diffusivity parameterization. We show that the parameterized eddy response to changing winds can qualitatively reproduce the observational findings and the results of eddy-resolving models.

## 2. Parameterizations of Baroclinic Eddies

[6] In the Gent and McWilliams [1990] (GM) parameterization, eddy transports are calculated as

$$\mathbf{u}^* = -\partial_z(K_{GM}\mathbf{S}) + \nabla_h \cdot (K_{GM}\mathbf{S})\mathbf{k}, \quad (1)$$

where  $\mathbf{u}^*$  is the bolus velocity,  $\mathbf{S} = -\nabla_h \varrho / \partial_z \varrho$  is the isopycnal slope,  $\varrho$  is the locally referenced potential density,  $\nabla_h$  is the horizontal gradient operator,  $K_{GM}$  is the thickness diffusivity, and  $\mathbf{k}$  is an upward-pointing unit vector.

[7] With a few exceptions [e.g., Griffies et al., 2005; Eden et al., 2008; Emile-Geay and Madec, 2009; Farneti et al., 2010],  $K_{GM}$  has a constant and uniform value in OGCMs. A more physical parameterization can be formulated following Larichev and Held [1995] and Visbeck et al. [1997], namely,

$$K_{GM} = \alpha L^2 \bar{\sigma}, \quad (2)$$

<sup>1</sup>Earth System Analysis, Potsdam Institute for Climate Impact Research, Potsdam, Germany.

<sup>2</sup>National Oceanography Centre, Natural Environment Research Council, Liverpool, UK.

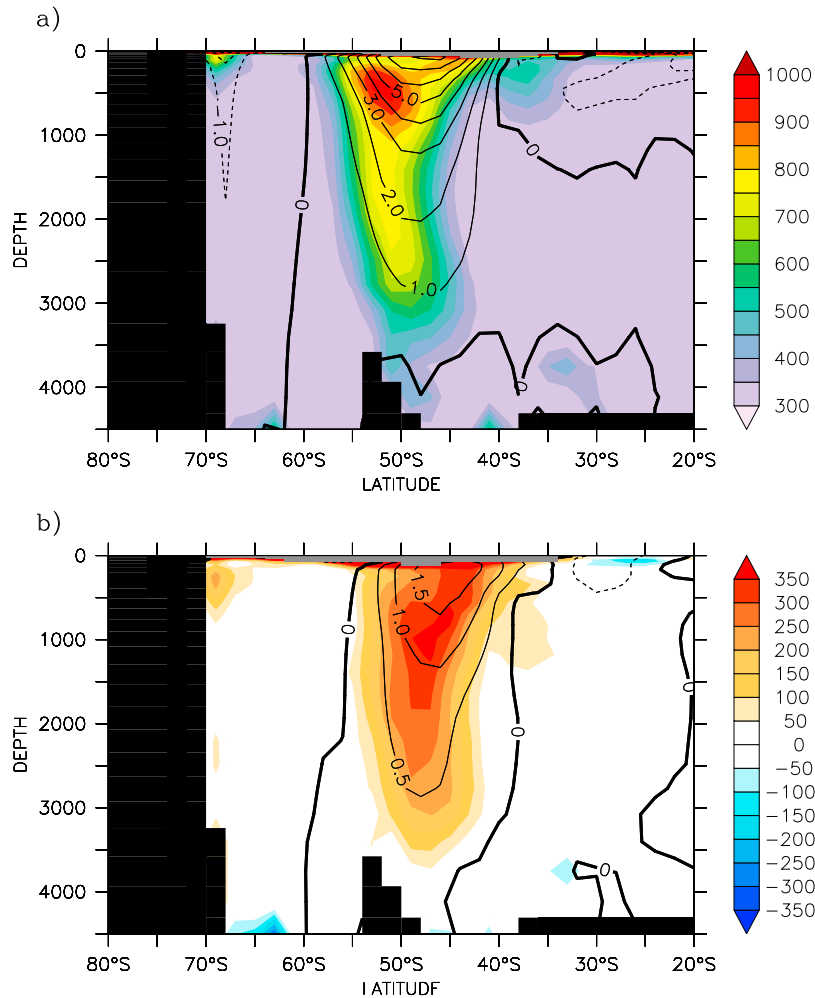


**Figure 1.** (a) Annual mean of  $K_{GM}$  zonally averaged between  $30^\circ$  W and  $30^\circ$  E for simulation **GM\_VAR** (in  $\text{m}^2\text{s}^{-1}$ ). The contours are the annual mean zonal currents (in  $\text{cm s}^{-1}$ ). (b) Changes in the fields depicted in Figure 1a at the end of the 200-year integration with ramped up winds.

where  $L$  is a mixing length,  $\bar{\sigma} = \sqrt{\bar{Ri}}^{-\frac{1}{2}}$  is the vertical average of the *Eady* [1949] growth rate, with  $\bar{Ri}$  the vertically averaged Richardson number and  $f$  the Coriolis parameter, and  $\alpha$  is a tuning parameter.

[8] The *Larichev and Held* [1995] and *Visbeck et al.* [1997] approaches only differ in their choice of  $L$ . While *Larichev and Held* [1995] used the baroclinic Rossby radius, *Visbeck et al.* [1997] proposed to take  $L$  as the maximum of the Rossby radius,  $L_R$ , the model grid size, and the width of the baroclinic zone. *Hallberg and Gnanadesikan* [2001] discussed the eddy flux scalings associated with the parameterizations of *Larichev and Held* [1995] and *Visbeck et al.* [1997], and concluded that the former performs better near eddy saturation, while the latter is most successful away from saturation. The simulations of *Bryan et al.* [1999] suggested, however, that the local Rossby radius might be the best choice for  $L$ .

[9] Values of  $K_{GM}$  diagnosed from eddy resolving models show that  $K_{GM}$  is not vertically uniform. In the Southern Ocean,  $K_{GM}$  attains values of  $1000\text{--}3000 \text{ m}^2 \text{ s}^{-1}$  in the upper 1000 m of the water column, but is ten times smaller in the deep. To account for this vertical structure, *Eden et al.* [2008] use a three-dimensional Richardson number  $Ri$  in their calculations of  $\sigma$ .

[10] In our numerical experiments, we use thickness diffusivities calculated according to (2), where, following *Bryan et al.* [1999],  $\alpha = 0.13$ ,  $L = L_R$  and  $\bar{\sigma}$  is replaced by  $\sigma = f Ri^{-\frac{1}{2}}$ . The diffusivity  $K_{GM}$  is not allowed to stray outside the interval  $[300, 30000] \text{ m}^2\text{s}^{-1}$ , but is otherwise permitted to vary in space and time. We use the quadratic tapering of *Gerdas et al.* [1991] with critical slope of 0.01 for the Redi diffusivity, and a similar, but linear, tapering with critical slope of 0.0025 for  $K_{GM}$ . Near the surface, both Redi and  $K_{GM}$  diffusivities are further tapered using the formulation of *Large et al.* [1997].

### 3. Model and Experimental Design

[11] The model consists of an OGCM based on the Modular Ocean Model version 3 coupled to an anomaly model of the atmospheric energy-moisture balance [*Hofmann and Morales Maqueda*, 2006]. The horizontal resolution is  $3^\circ \times 2^\circ$ . The model has 29 vertical levels with thickness increasing from 10 m at the surface to 405 m at the bottom. It incorporates a parameterization of bottom-enhanced vertical mixing [*Hasumi and Sugimoto*, 1999], with a vertical background diffusivity of  $10^{-5} \text{ m}^2\text{s}^{-1}$ . The vertical mixing scheme of *Large et al.* [1994] is used to represent

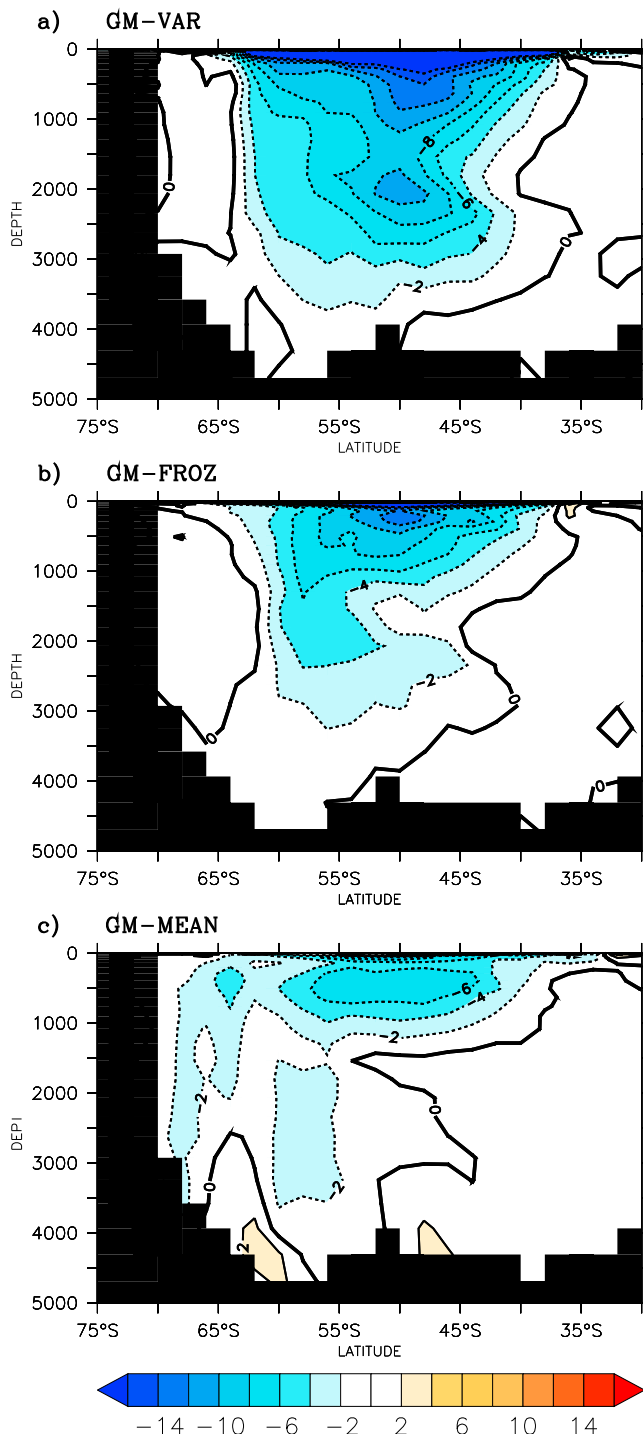


**Figure 2.** Change in the annual mean, meridional bolus transport (in Sv) at the end of the 200-year integration with ramped up winds: (a) **GM\_VAR**; (b) **GM\_FROZ**; and (c) **GM\_MEAN**.

turbulent effects in the mixed layer. Redi diffusivities are always equal to the 3-dimensional field of eddy thickness diffusivities, which is updated every time step. A second order moment tracer advection scheme greatly reduces the amount of spurious numerical diffusion and dispersion [Hofmann and

Morales Maqueda, 2006]. Climatological monthly mean wind stresses and all other atmospheric forcing were extracted from the NCEP/NCAR reanalysis data base [Kalnay *et al.*, 1996].

[12] The model was spun up for 3000 years. An annually averaged field of eddy thickness diffusivities was diagnosed from this spin-up. Subsequently, three 1000-year integrations were completed using as initial conditions the ocean state at the end of the spin-up. The first integration (**GM\_VAR**) was a continuation of the spin-up. In the second integration (**GM\_FROZ**), the eddy thickness diffusivity field was prescribed from the long-term annual mean of  $K_{GM}$  in the spin-up run. In the third integration (**GM\_MEAN**),  $K_{GM}$  was constant and spatially uniform, with a value of  $350 \text{ m}^2 \text{ s}^{-1}$ , the long-term annual mean of the global average of  $K_{GM}$  in the spin-up. To assess the model's sensitivity to wind changes, each 1000-year integration was continued for another 200 years, similarly to Farneti *et al.* [2010]. During the first 40 years of this 200-year period, the wind stress within the  $40^\circ \text{ S}$ – $80^\circ \text{ S}$  latitude band was ramped up linearly in time by 100% (an anomaly of size comparable to that of Farneti *et al.* [2010]). The wind stress was maintained at this anomalous level during the remaining 160 years of integration.

#### 4. Results and Discussion

[13] The climatological mean states of the **GM\_VAR** and **GM\_FROZ** simulations are very similar, and compare well with observations [Levitus and Boyer, 1994]. The maximum strength of the AMOC is 19.5 Sv ( $1 \text{ Sv} = 10^6 \text{ m}^3 \text{ s}^{-1}$ ), and the deep South Atlantic outflow at  $35^\circ \text{ S}$  is 17 Sv. The ACC transport is 80 Sv, with little interannual variability. This transport is too small, but consistent with simulations of other non-eddy resolving models. The baroclinic ACC transport between  $60^\circ \text{ S}$  and  $40^\circ \text{ S}$  (estimated from the meridional gradient of the baroclinic potential energy anomaly above 1900 m, as in work by Böning *et al.* [2008]) amounts to about 50 Sv, which is almost two thirds of the total ACC transport, in good agreement with the calculations of Böning *et al.* [2008].

[14] Before the wind stress anomaly is applied, the zonally integrated northward Ekman drift at the latitude of Cape Horn is 23.5 Sv. The parameterized eddy flow partly counteracts the Ekman drift, reducing the northward volume transport to 8.5 Sv. This eddy flow is largely concentrated in the upper 500 m.

[15] Figure 1a shows the annual mean of the  $K_{GM}$  field in simulation **GM\_VAR** zonally averaged between  $30^\circ \text{ W}$  and  $30^\circ \text{ E}$  before the southern hemisphere winds are ramped up. Superimposed to  $K_{GM}$  are the contours of the annual mean zonal current. In qualitative agreement with  $K_{GM}$  patterns diagnosed by Ferreira *et al.* [2005] and Eden *et al.* [2008], thickness diffusivities are largest in the general area of the ACC. However, there are significant differences in the spatial distribution of diffusivities, and we acknowledge that our results may be sensitive to these differences.

[16] The doubling of the wind stress in **GM\_VAR** causes an increase in  $K_{GM}$  of 25–50% in the area of the ACC (Figure 1b). There is also a strengthening of the ACC, which transports 115 Sv by the end of the simulation. The southward, annual mean meridional bolus transport in the upper 1900 m of the water column increases by 10 Sv (Figure 2a),

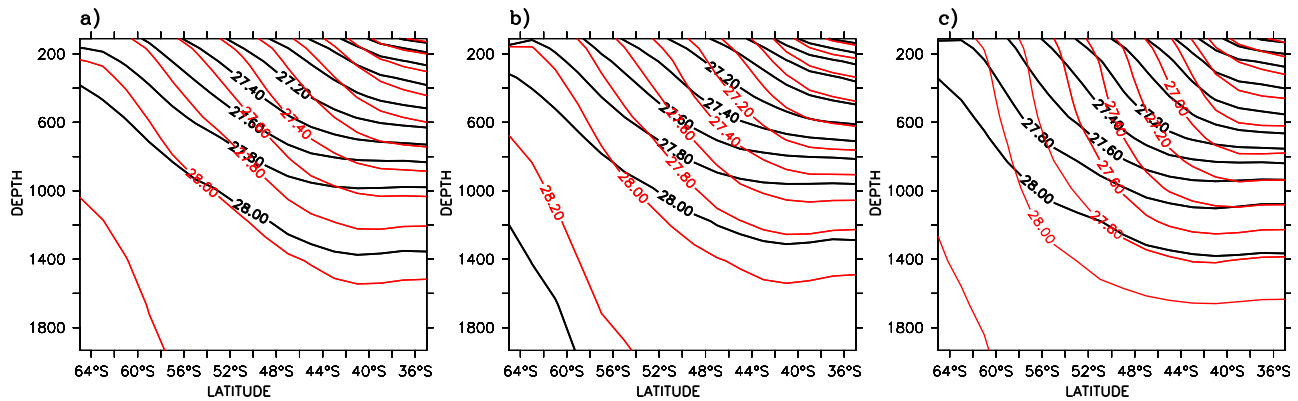


**Figure 3.** (a) Simulation **GM\_VAR**. Contours of annual mean  $\sigma_1$  zonally averaged between  $30^\circ$  W and  $30^\circ$  E before (black) and after (red) the increase in Southern Ocean westerlies at the end of the 200-year integration. (b and c) Same as Figure 3a but for **GM\_FROZ** and **GM\_MEAN**, respectively.

an increase caused directly by the steepening of the isopycnals and indirectly by the larger  $K_{GM}$  values. (Time series of the maximum value of  $K_{GM}$  in experiment **GM\_VAR** are shown in Figure S1.)<sup>1</sup> The meridional bolus transport also becomes stronger in simulations **GM\_FROZ** and **GM\_MEAN** after the wind stress is ramped up, but the increase is weaker and shallower than in **GM\_VAR** (Figures 2b and 2c). (Time series of the meridional bolus transport are shown in Figure S2.)

[17] The different responses of the meridional bolus transport in **GM\_MEAN**, **GM\_FROZ** and **GM\_VAR** are reflected in their corresponding isopycnal slope changes. Figure 3 shows how the annual mean contours of  $\sigma_1$  (potential density referred to a depth of 1000 m minus  $1000 \text{ kg m}^{-3}$ ) react to a doubling of the wind stress by the end of the simulation. The maximum slope of the  $\sigma_1 = 27.60 \text{ kg m}^{-3}$  increases by 30%, 66% and 70% in **GM\_VAR**, **GM\_FROZ** and **GM\_MEAN**, respectively. (A time series of the isopycnal slopes can be found in Figure S3.) The changes in the ACC baroclinic transport are, accordingly, much smaller in **GM\_VAR** ( $+22 \text{ Sv} \approx +44\%$ ) than in **GM\_FROZ** ( $+35 \text{ Sv} \approx +70\%$ ) and **GM\_MEAN** ( $+45 \text{ Sv} \approx +75\%$ ), which demonstrates the effectiveness of the eddy parameterization of **GM\_VAR** in stabilizing the ACC.

[18] Since ACC eddy dynamics should be a control of the AMOC [Gnanadesikan, 1999], we have also investigated the impact of the different eddy parameterizations on the response of the modeled AMOC to southern hemisphere wind variability. Figure S4 demonstrates indeed the importance that eddy compensation has for the modeled AMOC. In the same way as the ACC baroclinic transport response to the imposed wind perturbation is about double in **GM\_MEAN** than in **GM\_VAR** (**GM\_FROZ** is not shown), the accompanying increase in the AMOC is also almost twice as large in the former than in the latter.

## 5. Summary

[19] A sophisticated formulation of the *Gent and McWilliams* [1990] thickness diffusivity has allowed us to

simulate with some success the response of Southern Ocean eddies to changing midlatitude westerlies. An increase in the wind stress prompts a more vigorous northward Ekman transport and, hence, an initial steepening of the isopycnals. This steepening leads, in turn, to the creation of eddies that counteract the initial Ekman transport. The GM parameterization with constant and uniform eddy diffusivities is not able to appropriately represent this eddy compensation. We note that *Farneti et al.* [2010], with a vertically uniform formulation *à la Visbeck et al.* [1997] fail also to approach eddy compensation, partly because the *Visbeck et al.* [1997] formulation is less effective than the one by *Larichev and Held* [1995] near eddy saturation, but also because they use smaller maximum thickness diffusivities and capping isopycnal slopes than we do. Using an eddy diffusivity that is a function of the internal Rossby radius and the mean-flow Richardson number, a higher level of eddy compensation is attained. However, although the parameterized effective diffusivities attain maximum values comparable to those deduced from eddy-resolving simulations [e.g., *Marshall et al.*, 2006], the eddy formulation does not lead to levels of compensation as high as suggested by observations and eddy-resolving models.

[20] Because the enhanced negative eddy feedback in the model, the simulated ACC becomes less sensitive to wind stress changes, in qualitative agreement with observations [*Böning et al.*, 2008] and eddy-resolving models [*Farneti et al.*, 2010; *Hogg et al.*, 2008; *Hallberg and Gnanadesikan*, 2006]. The sensitivity of the AMOC to changes in the midlatitude westerlies of the southern hemisphere is also moderated by eddy compensation in the ACC, as expected from the theory of *Gnanadesikan* [1999]. Extrapolating from these results, we anticipate that, if full eddy compensation were attained, neither the ACC nor the AMOC would respond to such wind variability. However, eddy compensation should not be expected to hold for a large decrease in wind strength. Below a certain wind threshold, eddy activity will be too weak for compensation to occur, and the AMOC and the ACC should then become more sensitive to wind changes.

[21] **Acknowledgment.** M.H. was funded by the Deutsche Forschungsgemeinschaft (DFG), reference RA 977/5-1.

<sup>1</sup>Auxiliary materials are available in the HTML. doi:10.1029/2010GL045972.

## References

- Bi, D., W. F. Budd, A. C. Hirst, and X. Wu (2002), Response of the Antarctic circumpolar current transport to global warming in a coupled model, *Geophys. Res. Lett.*, *29*(24), 2173, doi:10.1029/2002GL015919.
- Böning, C. W., A. Dispert, M. Visbeck, S. R. Rintoul, and F. U. Schwarzkopf (2008), The response of the Antarctic Circumpolar Current to recent climate change, *Nat. Geosci.*, *1*, 864–869.
- Bryan, K., J. K. Dukowicz, and R. D. Smith (1999), On the mixing coefficient in the parameterization of bolus velocity, *J. Phys. Oceanogr.*, *29*, 2442–2456.
- Eady, E. T. (1949), Long waves and cyclone waves, *Tellus*, *1*, 33–52.
- Eden, C., M. Jochum, and G. Danabasoglu (2008), Effects of different closures for thickness diffusivities, *Ocean Modell.*, *26*, 47–59.
- Emile-Geay, J., and G. Madec (2009), Geothermal heating, diapycnal mixing and the abyssal circulation, *Ocean Sci.*, *5*, 203–217.
- Farneti, R., T. L. Delworth, A. J. Rosati, S. M. Griffies, and F. Zeng (2010), The role of mesoscale eddies in the rectification of the Southern Ocean response to climate change, *J. Phys. Oceanogr.*, *40*, 1539–1557.
- Ferreira, D., J. Marshall, and P. Heimbach (2005), Estimating eddy stresses by fitting dynamics to observations using a residual-mean ocean circulation model and its adjoint, *J. Phys. Oceanogr.*, *35*, 1891–1910.
- Fyfe, J. C., and O. A. Saenko (2006), Simulated changes in extratropical Southern Hemisphere winds and currents, *Geophys. Res. Lett.*, *33*, L06701, doi:10.1029/2005GL025332.
- Gent, P. R., and J. C. McWilliams (1990), Isopycnal mixing in ocean circulation models, *J. Phys. Oceanogr.*, *20*, 150–155.
- Gerdes, R., C. Köberle, and J. Willebrand (1991), The influence of numerical advection schemes on the results of ocean general circulation models, *Clim. Dyn.*, *5*, 211–226.
- Gnanadesikan, A. (1999), A simple theory for the thickness of the oceanic pycnocline, *Science*, *283*, 2077–2079.
- Griffies, S. M., et al. (2005), Formulation of an ocean model for global climate simulations, *Ocean Sci.*, *1*, 45–79.
- Hallberg, R., and A. Gnanadesikan (2001), An exploration of the role of transient eddies in determining the transport of a zonally reentrant current, *J. Phys. Oceanogr.*, *31*, 3312–3330.
- Hallberg, R., and A. Gnanadesikan (2006), The role of eddies in determining the structure and response of the wind-driven Southern Hemisphere overturning: Results from the modeling eddies in the Southern Ocean (meso) project, *J. Phys. Oceanogr.*, *36*, 2232–2252.
- Hasumi, H., and N. Sugimoto (1999), Effects of locally enhanced vertical diffusivity over rough bathymetry on the world ocean circulation, *J. Geophys. Res.*, *104*(23), 23,367–23,374.
- Hofmann, M., and M. A. Morales Maqueda (2006), Performance of a second-order moments advection scheme in an ocean general circulation model, *J. Geophys. Res.*, *111*, C05006, doi:10.1029/2005JC003279.
- Hogg, A. M., M. P. Meredith, J. R. Blundell, and C. Wilson (2008), Eddy heat flux in the Southern Ocean: Response to variable wind forcing, *J. Clim.*, *21*, 608–620.
- Jacobs, S. (1997), Observations of change in the Southern Ocean, *J. Phys. Oceanogr.*, *27*, 1849–1867.
- Kalnay, E., et al. (1996), The NCEP/NCAR 40-years reanalysis project, *Bull. Am. Meteorol. Soc.*, *77*, 437–471.
- Large, W. G., J. C. McWilliams, and S. C. Doney (1994), Oceanic vertical mixing: A review and a model with a nonlocal boundary layer parameterization, *Rev. Geophys.*, *32*, 363–403.
- Large, W. G., G. Danabasoglu, S. C. Doney, and J. C. McWilliams (1997), Sensitivity to surface forcing and boundary layer mixing in a global ocean model: Annual-mean climatology, *J. Phys. Oceanogr.*, *27*, 2418–2447.
- Larichev, V., and I. Held (1995), Eddy amplitudes and fluxes in a homogeneous model of fully developed baroclinic instability, *J. Phys. Oceanogr.*, *25*, 2285–2297.
- Levitus, S., and T. P. Boyer (1994), *World Ocean Atlas 1994*, vol. 4, *Temperature*, NOAA Atlas NESDIS, vol. 4, 129 pp., NOAA, Silver Spring, Md.
- Marshall, G. J. (2003), Trends in the Southern Annular Mode from observations and reanalysis, *J. Clim.*, *16*, 4134–4143.
- Marshall, J., E. Shuckburgh, H. Jones, and C. Hill (2006), Estimates and implications of surface eddy diffusivity in the Southern Ocean derived from tracer transport, *J. Phys. Oceanogr.*, *36*, 1806–1821.
- Rintoul, S. R., C. W. Hughes, and D. Olbers (2001), in *Ocean Circulation and Climate*, pp. 271–302, Academic Press, London.
- Saenko, A. O., J. C. Fyfe, and M. H. England (2005), On the response of the oceanic wind-driven circulation to atmospheric CO<sub>2</sub> increase, *Clim. Dyn.*, *25*, 415–426.
- Straub, D. N. (1993), On the transport and angular momentum balance of channel models of the Antarctic circumpolar current, *J. Phys. Oceanogr.*, *23*, 776–782.
- Thompson, A. F. (2008), The atmospheric ocean: Eddies and jets in the Antarctic Circumpolar Current, *Philos. Trans. R. Soc. A*, *366*, 4529–4541.
- Thompson, D. W. J., and S. Solomon (2002), Interpretation of recent Southern Hemisphere climate change, *Science*, *296*, 895–899.
- Toggweiler, J. R., and B. Samuels (1998), On the ocean's large scale circulation in the limit on no vertical mixing, *J. Phys. Oceanogr.*, *28*, 1832–1852.
- Toggweiler, J. R., K. Dixon, and K. Bryan (1989a), Simulations of radiocarbon in a coarse-resolution world ocean model: 1. Steady state pre-bomb distributions, *J. Geophys. Res.*, *94*(C6), 8217–8242.
- Toggweiler, J. R., K. Dixon, and K. Bryan (1989b), Simulations of radiocarbon in a coarse-resolution world ocean model: 2. Distributions of bomb-produced carbon 14, *J. Geophys. Res.*, *94*(C6), 8243–8264.
- Visbeck, M., J. Marshall, T. Haine, and M. Spall (1997), Specification of eddy transfer coefficients in coarse-resolution ocean circulation models, *J. Phys. Oceanogr.*, *27*, 381–402.
- Wunsch, C., and R. Ferrari (2004), Vertical mixing, energy and the general circulation of the oceans, *Annu. Rev. Fluid Mech.*, *36*, 281–314.

M. Hofmann, Earth System Analysis, Potsdam Institute for Climate Impact Research, Telegraphenberg A62, Potsdam D-14473, Germany. (hofmann@pik-potsdam.de)

M. A. Morales Maqueda, National Oceanography Centre, Natural Environment Research Council, Joseph Proudman Bldg., 6 Brownlow St., Liverpool L3 5DA, UK.